

1 Article

2 *Terminalia bentzoë*, a Mascarene endemic plant, 3 inhibits human hepatocellular carcinoma cells 4 growth *in vitro* via G0/G1 phase cell cycle arrest

5 Nawraj Rummun^{1,2,3}, Philippe Rondeau⁴, Emmanuel Bourdon⁴, Elisabete Pires⁵, James
6 McCullagh⁵, Timothy D.W. Claridge⁵, Theeshan Bahorun², Wen-Wu Li^{3*} and Vidushi S.
7 Neergheen^{1,2*}

8 ¹Department of Health Sciences, Faculty of Medicine and Health Sciences, University of Mauritius, Réduit,
9 80837, Republic of Mauritius. n.rajeevr10@gmail.com (NR); v.neergheen@uom.ac.mu (VSN)

10 ²Biopharmaceutical Unit Centre for Biomedical and Biomaterials Research, MSIRI Building, University of
11 Mauritius, Réduit, 80837, Republic of Mauritius. tbahorun@uom.ac.mu (TB)

12 ³School of Pharmacy and Bioengineering, Faculty of Medicine and Health Sciences, Thornburrow Drive,
13 Stoke on Trent, ST4 7QB, Keele University, UK. w.li@keele.ac.uk (WWL)

14 ⁴Université de La Réunion, INSERM, UMR 1188 Diabète athérombose Thérapies Réunion Océan Indien
15 (DéTROI), Saint-Denis de La Réunion, France. rophil@univ-reunion.fr (PR); emmanuel.bourdon@univ-reunion.fr (EB)

17 ⁵Chemical Research Laboratory, University of Oxford, Oxford, OX1 3TA, United Kingdom.
18 elisabete.pires@chem.ox.ac.uk (EP); james.mccullagh@chem.ox.ac.uk (JM); tim.claridge@chem.ox.ac.uk (TC)

19 * Correspondences: neergheen@uom.ac.mu (VSN); w.li@keele.ac.uk (WWL)

20 **Abstract:** Tropical forests constitute prolific sanctuary of unique floral diversity and potential
21 medicinal sources, however, many of them remain unexplored. The scarcity of rigorous scientific
22 data on the surviving Mascarene endemic taxa renders bioprospecting of this untapped resource of
23 utmost importance. Thus, in view of valorising the native resource, this study has as objective to
24 investigate the bioactivities of endemic leaf extracts. Herein, seven Mascarene endemic plants leaves
25 were extracted and evaluated for their *in vitro* antioxidant properties and antiproliferative effects on
26 a panel of cancer cell lines using MTT and clonogenic cell survival assay. Flow cytometry and comet
27 assay were used to investigate the cell cycle and DNA damaging effects, respectively. Bioassay
28 guided-fractionation coupled with LC-Mass spectrometry (MS), gas chromatography-MS, and
29 nuclear magnetic resonance spectroscopy analysis were used to identify the bioactive compounds.
30 Among the seven plants tested, *Terminalia bentzoë* was comparatively the most potent antioxidant
31 extract with significantly ($p < 0.05$) higher cytotoxic activities. *T. bentzoë* extract further selectively
32 suppressed the growth of human hepatocellular carcinoma cells and significantly halted the cell
33 cycle progression in G0/G1 phase, decreased the cells replicative potential and induced significant
34 DNA damage. Ten phenolic compounds including punicalagin and ellagic acid were identified and
35 likely contributed to the extract potent antioxidant and cytotoxic activities. These results established
36 a promising basis for further in-depth investigations on the potential use of *T. bentzoë* as supportive
37 therapy in cancer management.

38 **Keywords:** *Terminalia bentzoë*; Mascarene endemic; cytotoxicity; antioxidant; cell cycle arrest;
39 phenolics; bioassay-guided fractionation

40 1. Introduction

41 The plant kingdom is known to be a prolific sanctuary of phytochemicals with unique
42 therapeutic potential. At least 25 % of the 1562 clinical drugs approved by the US Food and Drugs
43 Administration are known to have been emanated from terrestrial plants [1,2]. Moreover, an estimate
44 of about 28187 plant taxa, globally, are documented to have medicinal values with over 3000 species
45 reported with the ethnomedicinal application against cancer [3,4]. The continued dependence of

46 mankind on plants was further evidenced during the recent outbreak of the COVID-19 pandemic
47 whereby, herbal medicines were used in an attempt to mitigate the symptoms of the novel
48 coronavirus infection [5–7].

49 Madagascar and its neighboring islands in the Western Indian Ocean regions are known as
50 biodiversity hotspots [8]. Undoubtedly, untapped endemic plant species from these niche areas
51 broadened the structural variation of novel chemotypes [9,10]. The tropical forest of Madagascar was
52 once acknowledged as a fertile source of economically valuable plants with pharmacologically active
53 ingredients [11]. Indeed, the anticancer drugs vinblastine and vincristine were derived from the
54 Madagascan endemic *Catharanthus roseus* (Apocynaceae) [12]. Certainly, the market value of
55 vincristine alone was estimated to be 15 million USD per kilogram, in the year 2016 [13].

56 Phylogeography investigations revealed that the Mascarene endemic plants islands have their
57 ancestral lineages traced back from Madagascar [14]. As such, the unique floral biodiversity of
58 Mauritius is expected to possess similar medicinal and therapeutic prolificacy as the Madagascan
59 rain forest. However, instead of conserving such valuable biodiversity, human activities are pushing
60 endemic taxa towards an unprecedented extinction crisis. In less than 400 years of human settlement,
61 Mauritius has witnessed the shrinking of its native forest to around 5 % of the original cover, leading
62 to the permanent loss of 30 (10.9 %) of its endemic plant species and driving 81.7 % of the remnant
63 endemic taxa on the brink of extinction [15–17]. For instance, fewer than 500 adults trees of *Terminalia*
64 *bentzoë* (L.) L.f. subsp. *bentzoë* is recorded in the wild, defining the species survival as vulnerable, as
65 per the IUCN red list criteria [18]. Nevertheless, the remnant areas of the pristine forest are still home
66 to a plethora of endemic flora rich in high genetic diversity representing interesting sources for
67 complementary and alternative medicine, nutraceuticals as well as pharmaceutical leads [16].

68 Initiation and progression of cancer are involved in oxidative stress via DNA damage and
69 increase of DNA mutations. Conventional chemo- and radiotherapy caused cancer cell death often
70 through generation of reactive oxygen species (ROS), but also unfortunately leading to severe side
71 effects. It is highly desired to develop more effective therapies with less toxic effects [19]. Plant
72 polyphenols exert anticarcinogenic activity by interfering with the different hallmarks of cancer,
73 including sustained tumor cell proliferation, angiogenesis and apoptotic cell death through various
74 signaling pathways [19,20]. Polyphenolics can also behave as antioxidants thereby maintaining the
75 integrity of DNA from oxidative stress attack and prevent the initiation stage of carcinogenesis
76 [21,22].

77 The tropical island of Mauritius is known for its endemic biodiversity richness [8]. However,
78 human activities on the island have provoked the irreversible loss of a considerable fraction of this
79 genetic resource. For instance, in less than four centuries, Mauritius has lost 95 % of its pristine forest
80 cover accounting for the extinction of 10.9 % of the island endemic flora [23]. The scarcity of rigorous
81 scientific data on the surviving endemic taxa renders bioprospecting of this untapped resource of
82 utmost importance. With this in mind, and in view of providing solid foundations to enforce stringent
83 conservation policies, the *in vitro* antioxidant propensities of leaf extracts from seven plants endemic
84 to Mascarene islands were investigated, in relation to their polyphenolic content. The plants under
85 study have documented traditional uses against ailments ranging from dermatological conditions,
86 asthma to infectious diseases (**Table 1**). The cytotoxic effect of *Terminalia bentzoë*, on a panel of cancer
87 cell lines, and its ability to impede the cell cycle progression in hepatocellular carcinoma (HepG2)
88 cells were determined. The bioactive constituents in *T. bentzoë* leaf extract were characterised
89 following bioassay-guided fractionation.

90 2. Materials and Methods

91 2.1. Plant material and preparation of total extracts.

92 Healthy fresh leaves of seven Mascarene endemic plants were collected in Mauritius and
93 deposited at the Mauritius herbarium, where plant species were authenticated by the botanist (Table
94 1). The leaves were air-dried followed by exhaustive maceration with aqueous methanol (80 %, v/v)
95 and freeze-dried as described previously [24]. The assay results were expressed in terms of the
96 lyophilised weight of extracts.

97 2.2. Estimation of polyphenolic contents.

98 The total phenolic, flavonoid, and proanthocyanidin level in the crude extracts were estimated
99 using the Folin-Ciocalteu assay, aluminium chloride assay and HCl/Butan-1-ol assay as described
100 [24].

101 2.3. *In-vitro* antioxidant capacities of extracts.

102 The antioxidant potential of the extracts was investigated according to reported methods [24,25].
103 Extract vehicle and gallic acid (or otherwise stated) were used as negative and positive controls
104 respectively. The percentage activity of the extracts was calculated relative to the negative control.
105 GraphPad Prism 6 software (GraphPad Inc., USA) was used to plot the dose-response curves and to
106 generate the half-maximal inhibitory concentration (IC_{50}) values. All experiments were performed in
107 triplicates in three independent assays. The results were expressed as mean \pm SEM.
108

109 2.3.1. Ferric reducing antioxidant potential assay

110 The final reaction volume of 3.4 mL of the ferric reducing antioxidant power assay contained 100 μ L
111 of extract and 300 μ L of water followed by addition of 3 mL FRAP reagent. The FRAP reagent was
112 prepared immediately before use by mixing 100 mL of 0.25 M acetate buffer (pH 3.6), 10 mL of 20
113 mM ferric chloride (source of Fe^{3+}) and 10 mL of 10 mM 2,4,6-tripyridyl-s-triazine. After incubating
114 the mixture for 4 minutes at ambient temperature, the absorbance was read at 593 nm against a blank.
115 Results were reported as in mmol Fe^{2+} .
116

117 2.3.2. 2,2-diphenyl-1-picrylhydrazyl (DPPH) assay

118 The DPPH assay protocol involved mixing varying concentrations, between 0 to 25 μ g/mL, of 100 μ L
119 of the methanolic extract with 200 μ L of 100 μ M methanolic DPPH and absorbance were read at 492
120 nm, 30 minutes post-incubation at ambient temperature.
121

122 2.3.3. Iron chelating assay

123 The reaction mixture for iron-chelating activity contained 40 μ L of plant extract (concentrations
124 between 0 to 10 mg/mL), 10 μ L of $FeCl_2 \cdot 4H_2O$ (0.5 mM) and 150 μ L of distilled deionized water. The
125 mixture was incubated at ambient temperature for 5 minutes, before the addition of 10 μ L of ferrozine
126 (2.5 mM) and the absorbance was read at 562 nm.
127

128 2.3.4. Superoxide scavenging assay

129 The final 250 μ L reaction volume for superoxide anion scavenging assay contained 25 μ L of
130 plant extract (concentrations between 0 to 300 μ g/mL), 100 μ L of 156 μ M of nitroblue tetrazolium and
131 100 μ L of 200 μ M beta-nicotinamide adenine dinucleotide reduced disodium salt hydrate and 30 μ L
132 of phenazine methosulphate. The absorbance was read at 560 nm following 30 minutes incubation at
133 25 °C.
134

Table 1. The investigated Mascarene endemic plant species.

Species	Family	Vernacular names	Ethnomedicinal uses [16]	Collection site	Collection date	Mauritius herbarium accession code	% Yield
<i>Antirhea borbonica</i> J.F.Gmel	Rubiaceae	Bois lousteau, Bois d'oiseau	Astringent, diarrhoea, dysentery, stop bleeding, promote wound repair, skin diseases, tambave, Urinary tract infections	Gaulettes Serrées	14-Oct-2014	MAU 0009462	5.53
<i>Dictyosperma album</i> (Bory) H. Wendl. & Drude ex Scheff var. <i>conjugatum</i> H. E. Moore & Guého	Arecaceae	Palmiste blanc	Not described	Réduit, Joseph Guého Arboretum	19-Aug-2014	MAU 0016674	8.52
<i>Erythroxyllum</i> <i>sideroxyloides</i> Lam	Erythroxyllaceae	Bois de ronde	Renal stones	Lower Gorges National Park, 'Morne Sec'	15-Oct-2014	MAU 0016542	13.81
<i>Ficus mauritiana</i> Lam <i>Hancea integrifolia</i> (Willd.) S.E.C. Sierra, Kulju & Welzen	Moraceae Euphorbiaceae	Figuier du pays Bois pigeon	Not described Clean the blood and improve blood circulation, tonic.	Gaulettes Serrées Gaulettes Serrées	14-Nov-2014 14-Nov-2014	MAU 0011002 MAU 0016431	3.10 10.42
<i>Stillingia lineata</i> Muell. Arg	Euphorbiaceae	Fangame; Bois de lait; Tanguin de pays	Eczema, skin disease	Lower Gorges National Park, 'Morne Sec'	27-Nov-2014	MAU 0016545	6.28
<i>Terminalia bentzoë</i> (L.) L.f. subsp. <i>bentzoë</i>	Combretaceae	Bois benjoin	Asthma, antipyretic, antimalarial, chills, dysentery, diarrhoea, depurative, emmenagogue, haemorrhages, Sexually transmissible diseases	Réduit, Joseph Guého Arboretum	7-Oct-2014	MAU 0016557	7.29

137 2.3.5. Nitric oxide scavenging assay

138 The nitric oxide radical scavenging activity was conducted in a 96-well plate. 50 μ L of aqueous
139 extract (0 to 100 μ g/mL) and 100 μ L of 5 mM of sodium nitroprusside (in phosphate saline buffer, pH
140 7.4) was incubated at 25 °C for 150 minutes. After incubation, 125 μ L of the reaction mixture was
141 transferred to another 96-well plate, to which 100 μ L of 0.33 % sulfanilic acid in 20 % glacial acetic
142 acid was added. After 5 minutes, 100 μ L of 0.1 % of N-1-naphthyethylenediamine dihydrochloride
143 was added and the pink coloration formed was read at 546 nm.

145 2.3.6. Deoxyribose degradation inhibitory assay

146 The deoxyribose degradation inhibitory assay protocol was optimised to a 24-well microtiter
147 plate format. Each well contained 50 μ L of aqueous extract, 50 μ L of 1 mM EDTA, 100 μ L of 500 μ M
148 FeCl₃, 50 μ L of 1 mM ascorbic acid, 50 μ L of 10 mM hydrogen peroxide, 100 μ L of 100 mM KH₂PO₄-
149 KOH buffer (pH 7.4) and 100 μ L of 15 mM 2-deoxyribose. The reaction mixture was incubated at 37
150 °C for 90 minutes. At the end of the incubation period, 500 μ L of 10 % (w/v) trichloroacetic acid
151 followed by 500 μ L of 1% (w/v) thiobarbituric acid were added to each well and the solutions were
152 heated in a water bath at 80 °C for 20 minutes to develop the pink chromogen. The absorbance of the
153 reaction mixture was read at 532 nm, both before and after incubation. Results were given in mg
154 lyophilised extract/mL.

155 2.4. Human cell lines and culture conditions

156 Human liposarcoma cells (SW872), human lung carcinoma cells (A549), human hepatocellular
157 carcinoma cells (HepG2), and human ovarian carcinoma cell lines OVCAR-4 and OVCAR-8 were
158 purchased from American Type Culture Collection (USA). Human ovarian epithelial (HOE) cells
159 immortalized using SV40 large T antigen was obtained from Applied Biological Materials Inc
160 (Canada). All cell lines, except the ovarian cell lines, were cultured in Dulbecco's Modified Eagle's
161 Medium. Roswell Park Memorial Institute (RPMI) 1640 medium was used in the case of ovarian cell
162 lines. Culture medium was supplemented with 10% fetal bovine serum, 2 mM L-glutamine and 100
163 U/L streptomycin-penicillin. Cells were grown in a humidified atmosphere of 5 % carbon dioxide
164 and 95 % humidity at 37 °C.

165 2.5. Cell-based assays

166 The viability of the investigated cells treated with test samples was evaluated using the methyl
167 thiazolyl diphenyl-tetrazolium bromide (MTT) cell viability assay. Following overnight
168 acclimatisation of cells in 96-well plate, cells were treated with test samples for 48 hours and assayed
169 for different parameters. For 96-well plate, the seeding densities for cancer cell lines and HOE cells
170 were 5 x 10³ cells and 2 x 10³ cells per well, respectively. All experiments were performed in triplicates
171 (unless otherwise specified) in three independent assays. To compare the chemotherapeutic potential
172 of the active extracts, the cytotoxicity of the extracts/purified compounds was evaluated against,
173 etoposide, a clinically used oncologic agent.

174 2.5.1. MTT viability assay

175 The MTT assay was performed as previously described [26]. The percentage cell viability relative
176 to DMSO control (0.025 % v/v, final concentration) was calculated and the IC₅₀ value determined
177 using GraphPad Prism 6 software (GraphPad Inc., USA).

178 2.5.2. Clonogenic cell survival assay

179 The effect of *T. bentzoë* leaf extract on the cell reproductive death was assessed by clonogenic cell
180 survival assay according to reported methods, with slight modifications [27,28]. HepG2 cells were
181 seeded in a 6-well plate (500/well) and allowed to attach overnight. Following 48 hours treatment
182 period with extract/ control, the media was replaced with fresh complete culture media and cells
183 were grown under standard recommended culture conditions for an additional 7 days to allow large

184 colonies formation. Colonies were then fixed with 4 % paraformaldehyde for 30 minutes and stained
185 with 0.5 % (w/v) crystal violet. The individual wells were imaged using a digital camera and the
186 colonies counted using ImageJ software (the US, National Institute of Health). The cytotoxic effect
187 was expressed as the percentage of surviving colonies relative to untreated control.

188 2.5.3. Single cell gel electrophoresis

189 Comet assay was carried out according to the method described [29,30] with minor
190 modifications. Briefly, 30 μ L of pre-treated cells were mixed with 70 μ L of 1 % (w/v) low melting
191 agarose (LMA) and 40 μ L of the cell-LMA mixture was placed on frosted microscope slides pre-
192 coated with 1.5 % normal melting agarose. A coverslip was placed on top of the cell-LMA mix and
193 allowed to solidify at 4°C for 1 hour in dark. Following solidification, the coverslip was gently slid
194 off and the slides were immersed in pre-chilled lysis buffer (2.5 M NaCl, 0.1 M EDTA, 10 mM Tris
195 base, 1% v/v Triton X-100 (added 30 minutes before use), pH 10, 4 °C) for 1 hour in dark. Following
196 this period, the excess lysis solution was drained and the slides were submerged in electrophoresis
197 buffer (0.2 M NaOH, 1 mM EDTA, pH 13, 4 °C) for 30 minutes in dark, to allow the DNA to unwind.

198 Electrophoresis was conducted for 30 minutes at 30 volts and 350 mA. The gels were neutralized
199 by immersing in pre-chilled neutralisation buffer (0.4 Tris-HCL, pH 7.5, 4 °C) for 10 minutes in dark.
200 The slides were washed in distilled water, fixed with 4 % formalin solution for 20 minutes and
201 allowed to air-dry overnight. The slides were stained with Hoechst 33342 (1 μ g/mL), air-dried in dark
202 and visualised at 200 X magnification in DAPI, using EVOS fluorescence microscope (Life
203 Technologies). Damaged DNA was measured for 100 randomly selected cells (for each independent
204 experiment) using the Comet Assay IV 4.3.1 (Perceptive instrument, UK).

205 2.5.4. Flow cytometric analysis

206 Apoptosis/necrosis analysis was performed on HepG2 cells after 48 hours treatment by flow
207 cytometry (Beckman Coulter's CytoFLEX and Cytexpert software) using Annexin V-FITC and
208 Propidium iodide (PI) double staining as described in a previous study [31]. Cell cycle analysis was
209 performed using propidium iodide for DNA staining as described [32]. Percentage of cells in different
210 phases (G_0/G_1 , S and G_2M phases) were quantified from propidium iodide fluorescence intensity-
211 area (PI-A) histograms corresponding to the DNA content of HepG2 cells.

212 2.5.5. MTT-guided fractionation and identification of bioactive molecules

213 The total extract of *T. bentzoë* was solubilised in distilled water and sequentially partitioned with
214 ethyl acetate, followed by n-butanol. Each fraction was dried and their cytotoxicity evaluated against
215 SW872, A549, HepG2 using the MTT cell viability assay. The butanol fraction being selective towards
216 HepG2 cells was subjected to Sephadex LH-20 column chromatography (30 cm X 2.1 cm internal
217 diameter) and eluted with water, water: methanol (3:1 v/v, 1:1 v/v and 1:3 v/v respectively), methanol
218 and acetone. The flow rate was maintained at 1.5 mL/min. Guided by the cytotoxicity against
219 HepG2 cells and purity profile, potent sub-fraction was further fractionated using semi-preparative
220 HPLC column. The crude extract and thereof derived purified fractions were analysed by extensive
221 spectroscopic methods including GC-MS, LC-MS, HPLC, 1H -NMR and ^{13}C -NMR (Supporting
222 Information). For analytical HPLC, the concentration of standards in the crude extract was
223 determined from the linear regression of the analytical standards curve namely $y = 12.317 x$, $R^2 =$
224 0.9996 : gallic acid and $y = 16.066 x$, $R^2 = 0.9992$: methyl gallate.

225 2.6. Statistical analysis

226 Statistical analyses were performed using GraphPad Prism 6 software (GraphPad Inc., San
227 Diego, California). The mean values among extracts were compared using One-Way ANOVA.
228 Student *t*-test and/or Tukey's multiple comparisons as Post Hoc test was used to determine
229 significances in mean phytochemicals, antioxidants and cytotoxic activities among different species.
230 All charts were generated using GraphPad Prism 6 software (GraphPad Inc., San Diego, California).

231 3. Results

232 3.1. Estimation of polyphenols level in the investigated leaf extracts.

233 The phenolic content varied significantly among the seven leaf extracts under study ($p < 0.05$)
234 with amounts ranging between 70.2 ± 4.72 mg and 385 ± 24.1 mg gallic acid equivalent/g. Total
235 flavonoid levels ranged between 2.43 ± 0.06 mg and 12.9 ± 0.45 mg quercetin equivalent/g. Based on
236 the spectrophotometric assay results, the estimated level of phenolics and flavonoids were
237 significantly highest ($p < 0.05$) in *T. bentzoë* leaf extract as compared to the other investigated leaf
238 extracts (**Table 2**). While the proanthocyanidin content prevailed in *E. sideroxyloides* leaf, both *S.*
239 *lineata* leaf and *T. bentzoë* leaf had a remarkably negligible amount of proanthocyanidin detected by
240 the butanol/HCl assay.

241 3.2. In-vitro antioxidant activities of the investigated leaf extracts.

242 An array of five analytical models was used to benchmark the antioxidant potential of the
243 investigated leaf extracts. The Mascarene endemic plant leaf extracts exhibited a varying degree of
244 activities in the different antioxidant assays. All extracts showed a dose-dependent metal chelating
245 and free radical scavenging activity (**Table 2**). In terms of iron chelation, all the extracts were weak
246 chelator compared to EDTA with an IC_{50} value of 0.01 ± 0.00 mg/mL (23.6 ± 0.22 μ M) ($p \leq 0.05$). As
247 depicted in **Table 2**, among the seven accessions of plants, *T. bentzoë* showed the most effective
248 antioxidant potential in all the five antioxidant assays. Thus, the free radical quenching activity of *T.*
249 *bentzoë* was further evaluated in hydroxyl radical scavenging assay. *T. bentzoë* ($IC_{50} = 0.25 \pm 0.03$
250 mg/mL) exhibited a significantly ($p < 0.0001$) greater degree of protection against Fenton-mediated
251 oxidative damage to 2-deoxyribose sugar moiety as compared to gallic acid ($IC_{50} = 1.65 \pm 0.09$ mg/mL).
252

253 3.3. Effect of *T. bentzoë* leaf extract on cell survival

254 To assess the antiproliferative properties of *T. bentzoë* leaf extract on cancer cells, first, the
255 influence of the extracts on the cell viability of five cancer cell lines notably, SW872, A549, HepG2,
256 Ovc4r-4 and Ovc4r-8 cells, were investigated using the MTT assay. *T. bentzoë* suppressed the growth
257 of all cancer cell lines in a dose-dependent manner. However, the dose of extract required to reach
258 the half-maximal inhibitory concentration differed considerably among the various cancer cell types.
259 The cytotoxicity of *T. bentzoë* was also evaluated against the non-malignant human ovarian epithelial
260 (HOE) cells and the IC_{50} value obtained (**Table 3**). HepG2 cells were more sensitive to *T. bentzoë*
261 treatment (selective index value 2.4 compared to HOE cells) (**Table 3**). At 48 hours of exposure, the
262 highest concentration of *T. bentzoë* extract (100 μ g/mL) reduced HepG2 cell viability to 20 % as
263 compared to untreated control cells (**Supplementary figure S1 A**). Subsequently, the effect of *T.*
264 *bentzoë* extract on the replicative ability of HepG2 cells was evaluated using the clonogenic cell
265 survival assay. *T. bentzoë* treatment significantly ($p < 0.0001$) reduced the number of surviving HepG2
266 colonies as compared to untreated control cells (**Figure 1**).

267

Table 2. Phenolic content and antioxidant potential of investigated leaf extracts.

Extract	Total phenolics ¹	Total flavonoids ²	Total proanthocyanidins ³	FRAP ⁴	Iron chelating activity ⁵	DPPH Scavenging activity ⁶	Superoxide scavenging activity ⁶	Nitric oxide scavenging activity ⁶
<i>A. borbonica</i>	70.2 ± 4.72 ^e	3.15 ± 0.07 ^{d,e}	5.71 ± 0.09 ^e	3.32 ± 0.16 ^{d,e,***}	4.05 ± 0.26 ^{b,c,***}	11.2 ± 1.63 ^{d,***}	19.0 ± 2.46 ^{d,***}	80.3 ± 29.0 ^{b,**}
<i>D. album</i>	75.7 ± 5.22 ^d	2.43 ± 0.06 ^f	30.9 ± 0.58 ^c	2.21 ± 0.05 ^{e,***}	4.83 ± 1.49 ^{c,d,***}	7.89 ± 0.13 ^{c,***}	32.7 ± 1.16 ^{f,***}	68.0 ± 10.0 ^{a,*}
<i>E. sideroxyloides</i>	182 ± 10.5 ^b	3.62 ± 0.13 ^d	121 ± 3.25 ^a	9.14 ± 0.85 ^{b,***}	1.46 ± 0.02 ^{a,***}	4.44 ± 0.26 ^{b,***}	12.7 ± 0.65 ^{c,***}	24.3 ± 1.39 ^a
<i>F. mauritiana</i>	133 ± 2.36 ^c	10.4 ± 0.21 ^b	85.7 ± 2.38 ^b	5.38 ± 0.01 ^{c,***}	0.43 ± 0.01 ^{a,***}	5.35 ± 0.23 ^{b,***}	24.2 ± 0.44 ^{e,***}	87.08 ± 28.9 ^{b,***}
<i>H. integrifolia</i>	142 ± 4.91 ^c	2.75 ± 0.06 ^{e,f}	18.4 ± 0.78 ^d	9.37 ± 0.29 ^{b,***}	0.78 ± 0.01 ^{a,***}	4.16 ± 0.16 ^{b,***}	9.55 ± 0.78 ^{b,***}	68.49 ± 37.5 ^{a,b,**}
<i>S. lineata</i>	97.7 ± 3.36 ^d	6.61 ± 0.19 ^c	ND	4.53 ± 0.02 ^{c,d,***}	6.45 ± 0.02 ^{d,*}	4.04 ± 0.17 ^{a,b,***}	3.81 ± 0.48 ^a	68.5 ± 42.9 ^{b,**}
<i>T. bentzoë</i>	385 ± 24.1 ^a	12.9 ± 0.45 ^a	ND	18.2 ± 0.01 ^{a,***}	0.10 ± 0.00 ^{a,***}	2.65 ± 0.14 ^{a,***}	5.20 ± 0.53 ^a	9.74 ± 3.13 ^a
Gallic acid	-	-	-	24.8 ± 0.22	8.00 ± 0.04 (47.0 ± 0.23 mM)	0.62 ± 0.05 (4.18 ± 0.32 µM)	5.52 ± 0.11 (31.4 ± 0.84 µM)	9.61 ± 1.75 (68.0 ± 13.9 µM)

268 ¹Values are expressed as mg of gallic acid equivalent (GAE)/g; ²values are expressed as mg of quercetin equivalent (QE)/g; ³values are expressed as mg of cyanidin
 269 chloride equivalent (CCE)/g; ⁴Values are expressed in mmol Fe²⁺; ⁵IC₅₀ values are expressed in mg/ml; ⁶IC₅₀ values are expressed in µg/ml; Data represent mean ±
 270 standard error of mean (n=3). ND = Not detected. Different letters between rows in each column represent significant differences between extracts (p < 0.05). Asterisks
 271 represent significant differences between extracts and gallic acid (positive control), * p ≤ 0.05, ** p ≤ 0.01, *** p ≤ 0.001, **** p ≤ 0.0001.

272

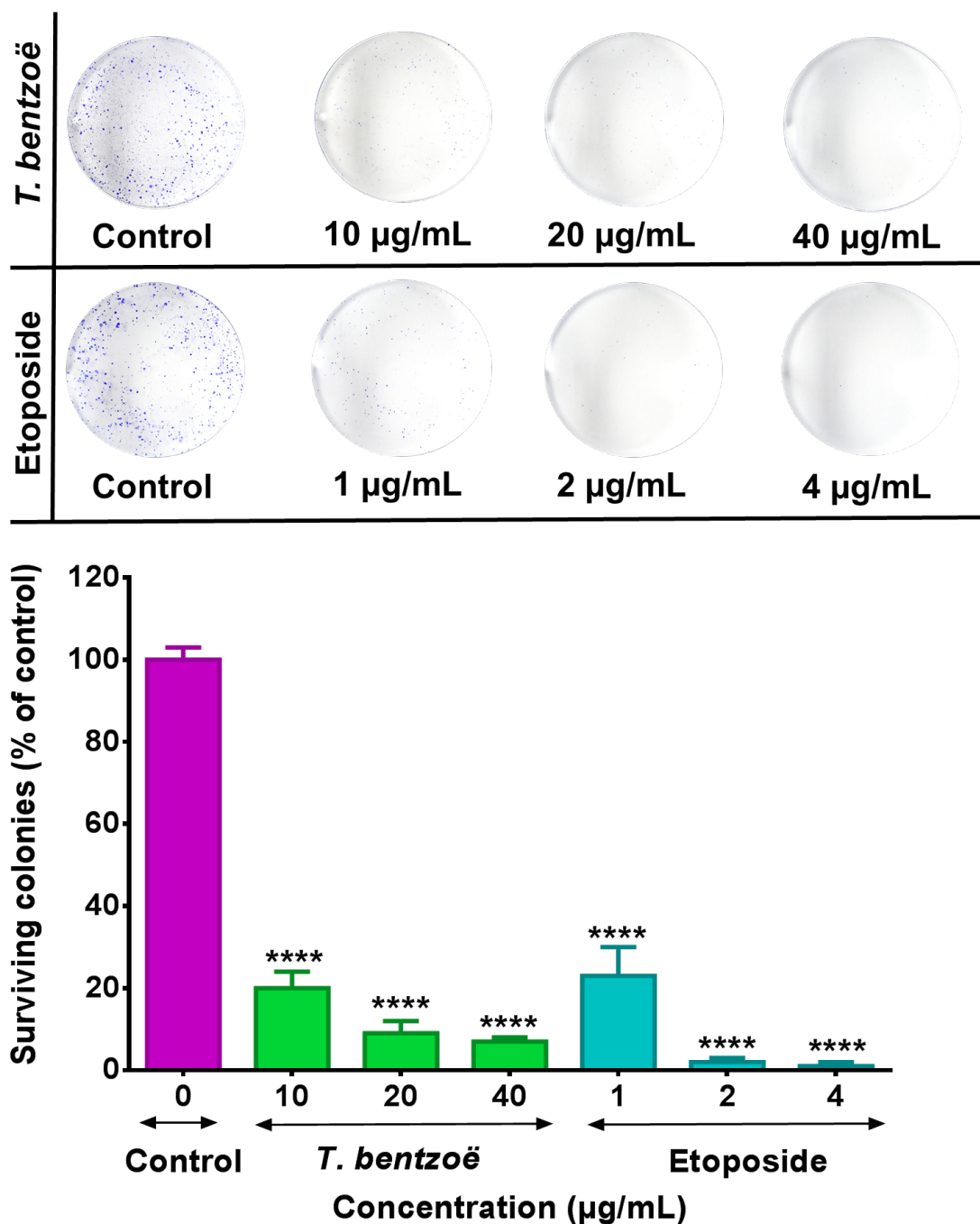
273

Table 3. Cytotoxicity (IC₅₀ µg/ml) of *T. bentzoë* against human cancer cell lines. .

Extracts	SW872	A549	HepG2	Ovcar-4	Ovcar-8	HOE
<i>T. bentzoë</i>	45.4 ± 1.8 ^{****}	96.8 ± 4.9 ^{****}	22.8 ± 1.3 ^{****}	30.1 ± 2.3	38.5 ± 4.2	55.5 ± 9.1
Etoposide	2.5 ± 0.2	6.8 ± 0.7	1.7 ± 0.2	NA	NA	1.5 ± 0.1

274

275 Data represent mean calculated IC₅₀ values with a standard error of the mean (n=3). NA= Etoposide at 1 µg/ml. Inhibited above 80 % cancer cell growth, indicating
 276 a much lower concentration is required for determination of IC₅₀ value. Asterisks represent significant differences between *T. bentzoë* and etoposide (positive control),
 277 **** p ≤ 0.0001.



278

279 **Figure 1.** HepG2 cells were treated with indicated concentrations (µg/mL) of test extracts for 48 hours
 280 and subsequently allowed to grow into colonies for 14 days. After 14 days, the colonies were stained
 281 with 0.1 % crystal violet and the images of the wells were captured using a digital camera. The
 282 colonies were counted using Image J software. Each experiment was performed three times. Asterisks
 283 represent significant differences between extracts treatments and untreated control, **** $p \leq 0.0001$.

284 3.3. Genotoxic effect of *T. bentzoë* extract in HepG2 cells.

285 DNA damage induced by *T. bentzoë* leaf extract was assessed in HepG2 cells by the alkaline
 286 comet assay. Treatment with 10 µg/mL *T. bentzoë* leaf extract for 24 hours resulted in the induction of
 287 significant ($p \leq 0.0001$) DNA damage in HepG2 cells as compared to untreated control cells. The
 288 occurrence of DNA damaged was scored in terms of tail length, tail intensity and olive tail moment
 289 of cell cultures by comet assay software (Table 4). The increased olive tail moment in response to *T.*

290 *bentzoë* treatment was 4-fold higher than that of untreated control cells. Cells treated with 200 μM
 291 H_2O_2 for 30 minutes, was used as a positive control.

292 **Table 4.** Tail length, tail intensity and olive tail moment of H_2O_2 and *T. bentzoë* treated HepG2 cells.

Extracts	Tail length (μm)	Tail intensity	Olive tail moment
Negative control (Culture medium)	32.8 ± 0.3	0.8 ± 0.1	0.2 ± 0.0
<i>Terminalia bentzoë</i>	$38.5 \pm 0.4^{****}$	$3.7 \pm 0.2^{****}$	$0.8 \pm 0.0^{****}$
Positive control (200 μM H_2O_2)	$90.8 \pm 7.2^{****}$	$46.8 \pm 2.6^{****}$	$14.1 \pm 0.6^{****}$

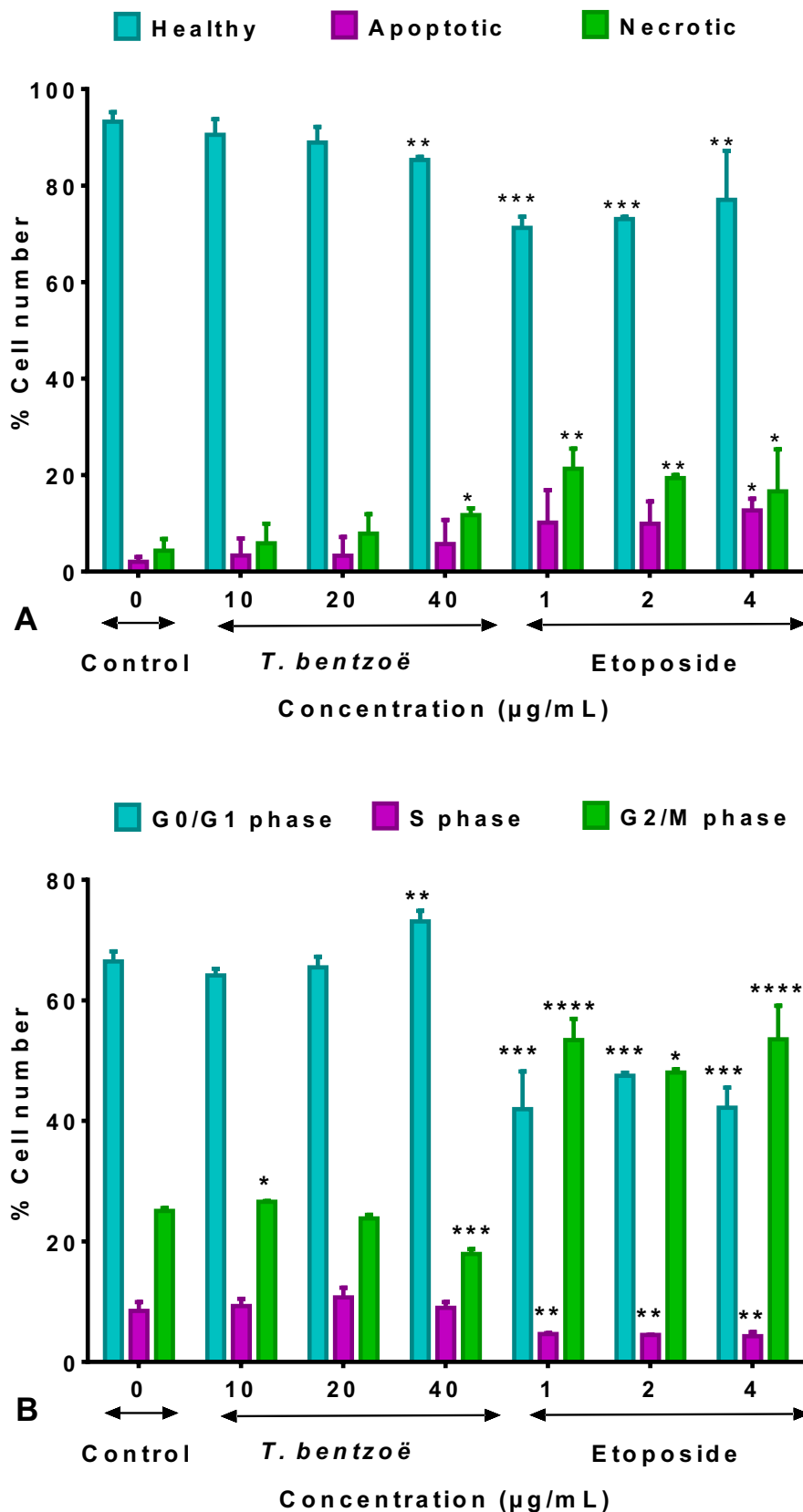
293 Asterisks represent significant differences between extracts and untreated control, **** $p \leq 0.0001$.

294 3.4. *T. bentzoë* induced cell death.

295 The proportion and distribution of HepG2 cells stained by annexin V-FITC and PI after 48 hours
 296 of exposure to *T. bentzoë* extract are illustrated in **figure 2A** and **supplementary figure S2**. The results
 297 indicated that, at a concentration equivalent to 10 $\mu\text{g}/\text{mL}$ and 20 $\mu\text{g}/\text{mL}$, the distribution pattern of
 298 the cell populations in the different quadrants (**supplementary figure S2**) is similar to that of DMSO
 299 control. However, exposure of HepG2 cells for 48 hours at 40 $\mu\text{g}/\text{mL}$, stimulated a significant increase
 300 in annexin V (1.41 fold, $p < 0.01$) and propidium iodide (1.52 fold, $p < 0.001$) fluorescence compared
 301 to the control. This increase is notably reflected in a higher percentage of necrotic cells necrotic cells
 302 (11.7%, $p < 0.01$) compared to the DMSO control (4.33%), indicating apoptotic/ necrotic cell death at
 303 this test concentration. Etoposide significantly ($p < 0.001$) increased the proportion of cells undergoing
 304 apoptosis (between 10 and 12 %)/ necrosis (between 16 and 21 %) at all three test doses, relative to
 305 DMSO control.

306 3.5. Cell cycle progression and *T. bentzoë*.

307 Flow cytometric analysis of DNA content, of HepG2 cells treated with test extracts for 48 hours,
 308 allowed the determination of the percentage of the cell population in each phase of the cell cycle. As
 309 emphasised in **figure 2B** and **supplementary figure S3**, exposure of HepG2 cells to 40 $\mu\text{g}/\text{mL}$ of *T.*
 310 *bentzoë* induced G0/G1 cell cycle arrest by increasing the cell population in G0/G1 (until $73.1 \pm 1.76\%$,
 311 $p < 0.01$ vs. ctrl) to the detriment of the G2/M phase (until $17.92 \pm 1.76\%$, $p < 0.001$ vs. ctrl). In contrast,
 312 treatment with 4 $\mu\text{g}/\text{mL}$ etoposide led to the accumulation of G2/M cell fraction (until $53.6 \pm 5.55\%$)
 313 to the detriment of G0/G1 cells fraction ($42.2 \pm 6.25\%$) suggesting G2/M arrest of HepG2 cell
 314 progression.



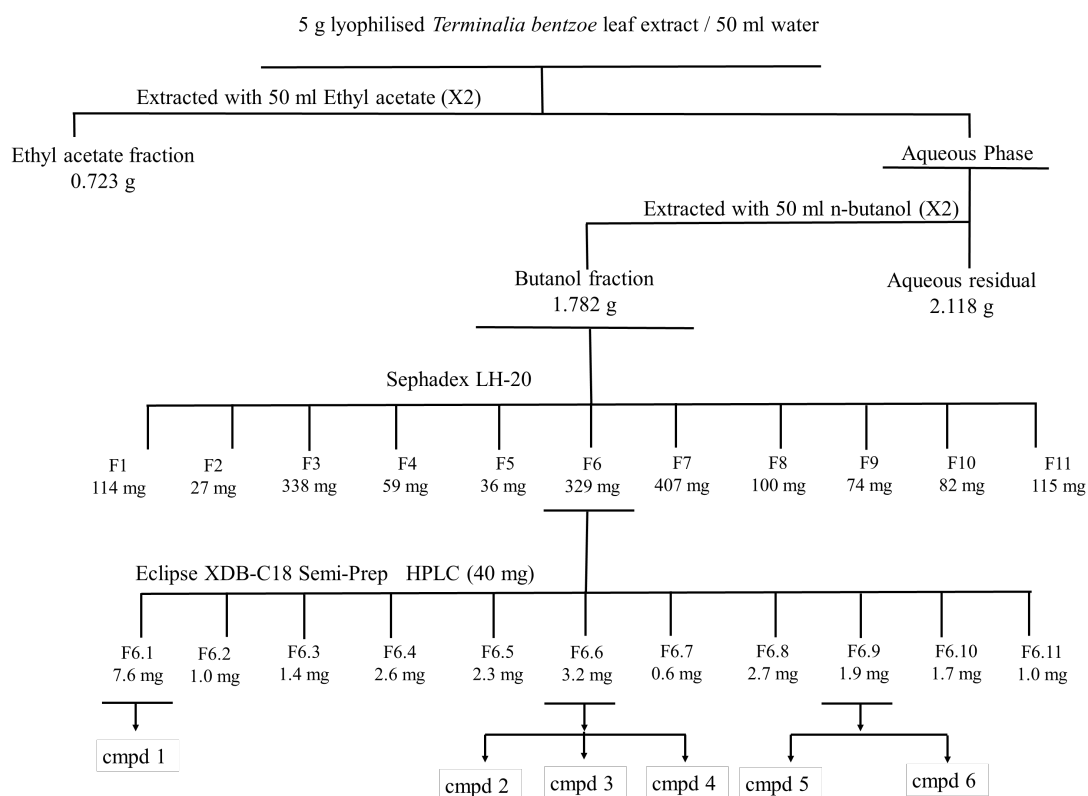
315

316 **Figure 2.** Effect of *Terminalia bentzoë* and etoposide on HepG2 cells as analysed by flow cytometry. (A)
 317 Annexin V-FITC/PI staining of HepG2 cells after 48 hours treatment and (B) cell cycle progression.
 318 Apoptosis and necrosis levels are expressed as percentage of the total cell population and given as mean \pm SD
 319 (n=5). Percentage of cells in different phases (G0/G1, S and G2/M phases) are expressed as mean \pm SD
 320 (n=3). Asterisks represent significant differences between test concentrations and DMSO control. * $p \leq 0.05$,
 321 ** $p \leq 0.01$, *** $p \leq 0.001$, **** $p \leq 0.0001$.

322 3.5. Bioassay guided fractionation of *T. bentzoë* leaf extract323 3.5.1. Effect of *T. bentzoë* fractions on HepG2 cell viability

324 HepG2 cells were used as a model to fractionate and characterise the bioactive components
 325 present in *T. bentzoë* leaf extract. The first round of fractionation was achieved using liquid-liquid
 326 partitioning with organics solvents of increasing polarities. *T. bentzoë* butanol fraction, being most
 327 active, was further fractionated on a Sephadex LH-20 column. A total of 11 sub-fractions was derived
 328 with cytotoxic activity being limited between fractions F4 to F10 only (Table 5). Assessment of their
 329 chromatographic patterns revealed differences in the chemical compositions of the fractions, albeit
 330 multiple overlapping peaks highlighting the chemical complexity of the subfractions. Given the most
 331 potent cytotoxic activity of the subfraction F6 ($IC_{50} = 15.2 \pm 1.8 \mu\text{g/mL}$), the further fractional
 332 separation of the latter was achieved using preparative HPLC to yield 11 HPLC subfractions (F6.1 –
 333 F6.11). Of these, HPLC subfraction F6.1 retained most of the cytotoxic activity, providing an IC_{50} value
 334 of $15.8 \pm 0.3 \mu\text{g/mL}$. By contrast, HPLC fractions F.2, F.7, F.9, F.10 and F.11 failed to effectively inhibit
 335 the growth of HepG2 cell cultures; hence no IC_{50} values were determined for these subfractions. A
 336 summary of the bioassay-guided fractionation employed is depicted in figure 3.

337



338

339 **Figure 3.** MTT- guided fractionation of *T. bentzoë* extract cytotoxicity against HepG2 cells. Compd:
 340 Compound. Compd 1= α and β - Punicalagin; compd 2= Isoterchebulin; compd 3 = Terflavin A; compd 4
 341 = 3,4,6-trigalloyl- β -D-glucopyranose, compd 5 = 2''-O-galloyl-orientin; compd 6 = 2''-O-galloyl-
 342 isoorientin.

343 3.5.2. Antioxidant potential of *T. bentzoë* fractions

344 Both the ethyl acetate ($22 \pm 0.29 \text{ mmol Fe}^{2+}$) and butanol ($21.01 \pm 0.56 \text{ mmol Fe}^{2+}$) fractions were
 345 significantly ($p \leq 0.05$) higher compared to the aqueous residual fraction. Furthermore, the FRAP
 346 value of the organic fractions was greater as compared to the total extract. The butanol fraction of *T.*
 347 *bentzoë* was a more effective scavenger of DPPH• radical as opposed to ethyl acetate and aqueous

348 residual fractions (**Table 5**). As far as the butanol subfractions were concerned, notably F6, F7, and
349 F8 had better antioxidant activity in FRAP and superoxide radical scavenging assays (**Table 5**).

350 3.6. Characterisation of the cytotoxic components of *T. bentzoë*.

351 In an effort to identify the bioactive constituents in *T. bentzoë*, bioassay-guided fractionation was
352 carried out. LC-MS analysis in conjunction with NMR spectroscopy of *T. bentzoë* butanol fraction 6
353 and its semi-prep HPLC sub-fractions allowed the identification of 8 phenolic compounds including
354 α and β -punicalagin (**1**), isoterchebulin (**2**), terflavin A (**3**), 3,4,6-trigalloyl- β -D-glucopyranose (**4**), 2''-
355 O-galloyl-orientin (**5**), 2''-O-galloyl-isoorientin (**6**), 2''-O-galloylvitexin (**7**), and ellagic acid (**8**) (**Figure**
356 **4**, **Table 6**, **Supplementary Figures S4**). The bioactive HPLC subfractions F6.1 (IC_{50} value = 15.8 ± 0.3
357 $\mu\text{g/mL}$) revealed to be α and β - punicalagin (**1**) (**Supplementary Figures S5**), while a mixture of
358 isoterchebulin (**2**), terflavin A (**3**), and 3,4,6-trigalloyl- β -D-glucopyranose (**4**) (**Supplementary Figures**
359 **S6**) was identified from the active subfraction F6.6 (IC_{50} value = $19.6 \pm 0.7 \mu\text{g/mL}$). A mixture of 2''-O-
360 galloyl-orientin (**5**) and 2''-O-galloyl-isoorientin (**6**) (**Supplementary Figures S7 and Table S1**), with
361 a ratio of 5:2 based on the ^1H NMR integration of single hydrogen in each compound was identified
362 from the non-active subfraction F6.9. 2''-O-galloylvitexin (**7**), and ellagic acid (**8**) were detected only
363 by LC-MS from the butanol fraction 6 (**Supplementary Figures S4**). Additionally, two simple
364 phenolics, gallic acid and methyl gallate were detected in both the ethyl acetate and butanol fractions
365 and identified by GC-MS analysis (**Supplementary figure S8**). They were likely present in other less
366 bioactive fractions. The levels of gallic and methyl gallate were quantified as 15.6 ± 1.1 and 26.2 ± 8.1
367 $\mu\text{g/mg}$ total extract) ($n=3$) by HPLC, respectively.

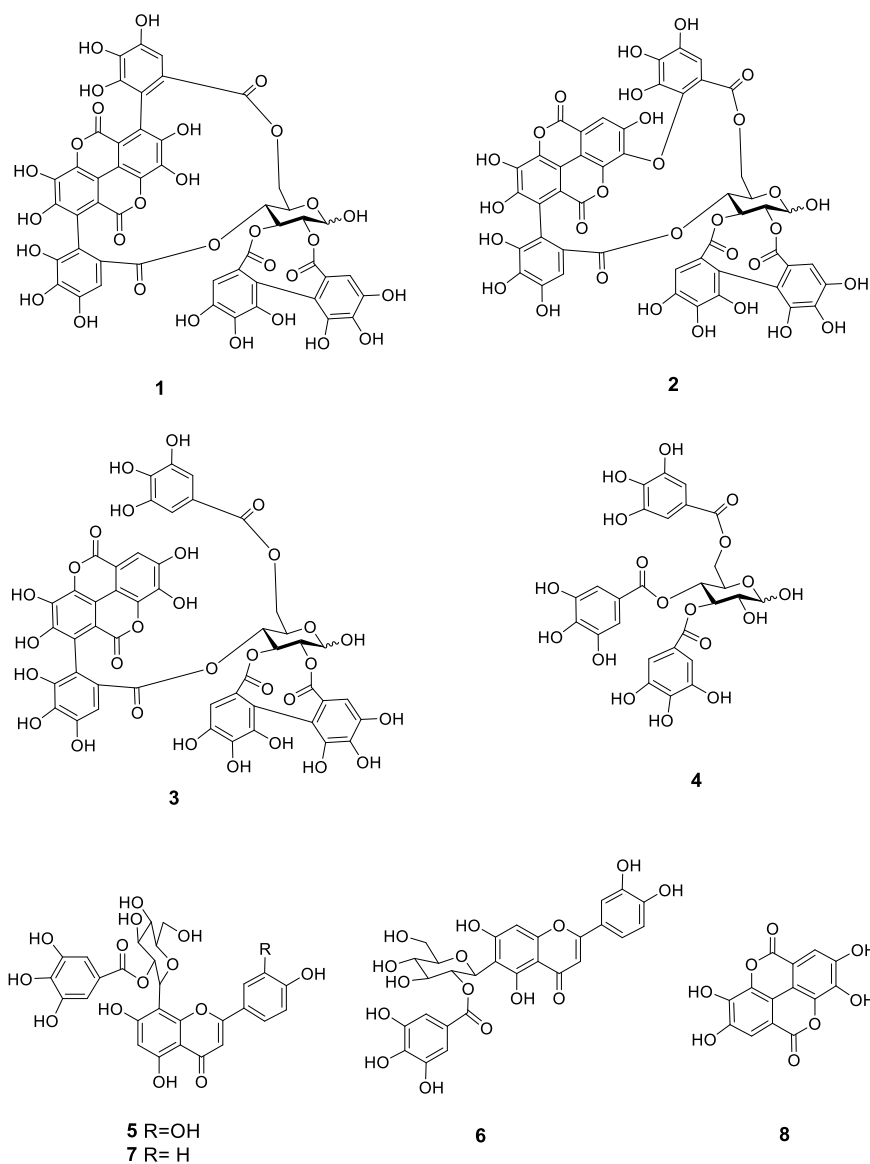


Figure 4. Chemical structure of polyphenolic compounds (1-8) identified in *Terminalia bentszoi* L. leaf extract.

368

369

370

371

372
373**Table 5.** Cytotoxic and antioxidant potential of *T. bentzoë* leaf fractions and the isolated punicalagin (1).

<i>T. bentzoë</i> Fractions		<i>IC</i> ₅₀ ($\mu\text{g/mL}$) against HepG2 cells	FRAP ¹	DPPH ²	Superoxide scavenging activity ²
Ethyl acetate		20.8 \pm 0.1	21.98 \pm 0.29 ^{a,b}	1.17 \pm 0.02 ^{d,e}	7.43 \pm 0.14 ^b
Butanol		18.3 \pm 3.4	21.01 \pm 0.56 ^{b,c}	0.98 \pm 0.06 ^e	7.65 \pm 0.10 ^b
Aqueous residual		26.8 \pm 5.5	15.29 \pm 0.16 ^e	1.78 \pm 0.07 ^{b,c}	10.70 \pm 0.20 ^{a,b}
T. bentzoë butanol subfractions	F1	ND	3.04 \pm 0.10 ^g	ND	ND
	F2	ND	13.62 \pm 0.16 ^f	2.65 \pm 0.04 ^a	16.90 \pm 0.35 ^a
	F3	ND	13.80 \pm 0.14 ^{e,f}	1.79 \pm 0.12 ^{b,c}	10.80 \pm 0.28 ^{a,b}
	F4	28.9 \pm 1.5	14.42 \pm 0.27 ^{e,f}	2.09 \pm 0.08 ^b	8.96 \pm 0.12 ^b
	F5	25.7 \pm 2.9	18.46 \pm 0.15 ^d	1.71 \pm 0.07 ^c	8.71 \pm 0.10 ^b
	F6	15.7 \pm 1.8	23.01 \pm 0.68 ^a	1.19 \pm 0.09 ^{d,e}	7.03 \pm 0.20 ^b
	F7	19.9 \pm 4.7	20.94 \pm 0.49 ^{b,c}	1.01 \pm 0.07 ^{d,e}	7.15 \pm 0.18 ^b
	F8	24.6 \pm 5.9	19.86 \pm 0.29 ^{c,d}	1.12 \pm 0.06 ^{d,e}	8.76 \pm 0.08 ^b
	F9	22.3 \pm 3.1	18.82 \pm 0.31 ^d	0.99 \pm 0.06 ^e	9.33 \pm 0.24 ^b
	F10	26.7 \pm 6.2	18.47 \pm 0.28 ^d	1.34 \pm 0.04 ^d	9.05 \pm 0.23 ^b
	F11	ND	0.09 \pm 0.02 ^h	ND	ND
Active HPLC subfractions	F6.1 (Punicalagin (1))	15.8 \pm 0.3	-	-	-
	F6.3	27.5 \pm 0.8	-	-	-
	F6.4	17.4 \pm 0.4	-	-	-
	F6.5	22.1 \pm 0.6	-	-	-
	F6.6	19.6 \pm 0.7	-	-	-
	F6.8	18.6 \pm 0.4	-	-	-

374

375
376
377
378

¹Values are expressed in units of mmol Fe²⁺/gFDW; ²Values are expressed in units of $\mu\text{g/mL}$; Data represent mean with a standard error of the mean (n=3). Different letters between rows in each column represent significant differences between extracts ($p < 0.05$). ND = *IC*₅₀ value not reached at maximum test dose. "-" = Not tested.

379
380**Table 6.** Identification of phenolic compound in *T. bentzoë* butanol fraction F6 using high-resolution mass spectrometry, NMR spectroscopy, and comparison with literature and available data.

Compound number	RT/min	Negative ESI-MS [M-H] ⁻	Molecular formula	Compound	References
1	0.76	1083.0555	C ₄₈ H ₂₈ O ₃₀	Punicalagin	[33–36]
2	4.08	1083.0555	C ₄₈ H ₂₈ O ₃₀	Isoterchebulin	[33]
3	4.58	1085.0710	C ₄₈ H ₃₀ O ₃₀	Terflavin A	[37]
4	4.97	635.0867	C ₂₇ H ₂₄ O ₁₈	3,4,6-trigalloyl- β -D-glucopyranose	[38]
5	6.25	599.1017	C ₂₈ H ₂₄ O ₁₅	2''-O-galloyl-orientin	[34]
6	6.25	599.1017	C ₂₈ H ₂₄ O ₁₅	2''-O-galloyl-isoorientin	[34]
7	6.53	583.1074	C ₂₈ H ₂₄ O ₁₄	2''-O-Galloylvitexin	[34,35]
8	6.72	300.9987	C ₁₄ H ₆ O ₈	Ellagic acid	[33]

381 4. Discussion

382 Medicinal plants are known to be the epicentre of numerous well established ethnomedicinal
383 systems across the globe [4]. However, more than 84 % of these medicinal plants have been poorly
384 studied in regards to their phytochemical compositions, clinical efficacy as well as their safety and
385 toxicological profiles [4]. Moreover, forest cover is being uprooted across the world, at an
386 unprecedented rate, threatening the survival of at least 15000 medicinal plant species [39]. Plant
387 secondary metabolites have contributed enormously to the modern-day pharmaceutical industry by
388 providing the chemical backbone for almost 25 % of the 1562 clinical agents as well as 60 % of the 246
389 oncologic drugs approved by the US Federal Drugs Administration between 1981 and 2014 [1,2,40].
390 As such it is of utmost importance to evaluate the unexplored terrestrial flora for their therapeutic
391 potential, as the dwindling medicinal plant's species continues to stand as a rich repository to probe
392 for novel chemotypes in the drug developmental process.

393 The current findings highlighted the richness of the different subclasses of polyphenolics,
394 notably phenolics, flavonoids and proanthocyanidins, the distribution of which differed significantly
395 ($p < 0.05$) among the investigated accessions (Table 2). The biosynthesis of flavonoids, in particular
396 flavonols, are known to be upregulated in response to ultra-violet radiation [41]. The accumulation
397 of flavonoids in the endemic plant leaves collected from Mauritius may be attributed to the high
398 sunlight conditions and UV radiation which are characteristic to tropical islands like the Mascarene
399 [42].

400 Given the ubiquitous involvement of oxidative damage in carcinogenesis, antioxidant-rich
401 secondary metabolites, notably, polyphenolics have attracted much interest in the search of novel
402 and alternative treatment modalities for cancer [43,44]. In this vein, the *in vitro* antioxidant activities
403 often correlated strongly with the growth inhibitory activity against cancer cell lines [45,46].
404 However, it is crucial to note that both ROS and antioxidants have a "Janus-faced" effect in cancer
405 management, as their effect differs in the early events of cancer initiation, from those involved in the
406 survival and propagation of an establish tumors [43,47]. On one hand, where moderate ROS level
407 promotes the transformation of a normal cell to malignant cells, elevating the ROS level in cancer
408 cells beyond the cell tolerance threshold may promote oxidative stress-induced cell cytotoxicity [47–
409 49]. It should be noted that many standard chemotherapies cause cancer cell death via generation of
410 ROS and excessive oxidation [50], therefore the effect of antioxidant polyphenols in combination with
411 these chemotherapies on cancers must be fully evaluated *in vitro* and *in vivo* before use in patients.

412 The antioxidant mechanism of action of polyphenols are multifaceted, thus a panel of *in vitro*
413 assay models allowed to gauge the antioxidant potential of the evaluated extracts [51]. *T. bentzoë*
414 having the highest abundance of total phenolics and flavonoids also exhibited the most potent
415 antioxidant activity in all six *in vitro* assays and was further evaluated for its cytotoxicity against
416 cancer cell lines. However, the other six plant species might also show cytotoxicity through different
417 mechanisms, which were not investigated in this study.

418 The cytotoxicity of different *Terminalia* species against multiple cancerous cell lines is
419 documented. Investigation of the cytotoxic activity of methanolic leaf extracts of *T. arjuna* against
420 human chronic myelogenous leukaemia cells led to the isolation of the bioactive ursolic acid
421 (triterpenoid) [52]. Leaf extracts of *T. chebula* suppressed the growth of human breast and lung cancer
422 cell lines [53]. Along a similar line, the leaf extract from *T. catappa* significantly ($p < 0.05$) suppressed
423 the proliferation of human colorectal (SW480) cell line in a dose-dependent manner by
424 downregulating the level of B-cell lymphoma 2 (BCL-2) gene expression while upregulating the level
425 of Caspase 9 and Caspase 3, indicative of the mitochondrial pathway of apoptosis in SW480 cells [54].

426 The foremost aim of oncologic agents is to precisely target cancerous cells with minimal effect
427 on non-malignant cells. *T. bentzoë* crude extract had a selective index value of approximately 2.5,
428 indicating that the extract had some degree of selectivity towards HepG2 cells as opposed to non-
429 malignant human ovarian epithelial cells. Nevertheless, it is crucial to also assess the cytotoxicity of
430 the extract against a panel of normal cells of different tissue origins, to provide greater insight
431 regarding its toxicity window and safety profile.

432 In line with the United States National Cancer Institute cytotoxicity guidelines [55,56], *T. bentzoë*
433 crude extract with an IC_{50} value of $22.8 \pm 1.3 \mu\text{g/mL}$ can be considered as a potent candidate for further
434 investigation with regards to its anticancer potential. It is known that, following exposure to
435 toxicants, a subpopulation of cells enters a dormant state. These dormant viable cells further retained
436 their ability to replicate into stem-like progeny cells which might lead to the development of drug-
437 resistance and cancer relapse [57,58]. Thus, while investigating the potential anticancer effect of
438 extracts, it is warranted to also evaluate their long-term effect on the replicative ability of the cancer
439 cell line. The colony formation assay is a simple and useful *in vitro* model, considered as the gold
440 standard to predict the long-term sensitivity of cancer cell response to therapeutics treatment [57,59].
441 In this vein, the current study evidenced the ability of *T. bentzoë* to impede the replicative potential
442 of HepG2 cells (**Figure 1**). Numerous anticancer agents, including polyphenols, are known to
443 abrogate the limitless replicative ability of different cancer cell variants [60,61]. Catechin, catechin-3-
444 O-gallate, 7-O-galloyl catechin, and methyl gallate purified from *Acasis hydaspica* is reported to
445 suppress the long-term clonal proliferation of prostate cancer (PC-3) cells [62].

446 This study also attempted to delineate the mode of *T. bentzoë* induced HepG2 cell death. Flow
447 cytometric analysis of annexin V-FITC and PI dual stained HepG2 cells treated with $40 \mu\text{g/mL}$,
448 revealed a significant ($p < 0.05$) increased in both Annexin V-FITC and PI fluorescence level,
449 compared to the untreated control, thus indicating the putative activation of both apoptotic and
450 necrotic pathways in HepG2 cells. Cells grown as monoculture are known to initiate apoptosis which
451 is terminated by necrosis like events, also termed as secondary necrosis, due to the absence of
452 phagocytic scavenger cells [63,64]. Numerous studies evidenced this type of cancer cell death
453 following treatment with cytotoxic agents. Ellagic acid was reported to induce both apoptotic and
454 necrotic cell death mechanism in human pancreatic cancer cell cultures [65]. A similar effect of
455 *Lepidium sativum* and *Vitis vinifera* extract were highlighted in human breast and skin cancer cells,
456 respectively [66,67].

457 Plant extracts and/or thereby derived phytochemicals are known to provoke cancer cell death
458 by causing oxidative damage to genetic material mediated cell cycle arrest and subsequent cell death
459 [68,69]. With this in mind, the DNA damage to HepG2 cellular DNA following *T. bentzoë* crude
460 extracts treatment was investigated using the alkaline comet assay and scored in terms of tail length,
461 tail intensity, and olive tail moment. The comet assay is a well-established and highly sensitive
462 method for the detection of DNA damage and fragmentation pattern [70]. *T. bentzoë* induced 4 folds
463 significantly ($p < 0.001$) higher DNA damaged to HepG2 cells compared to the untreated control, as
464 reflected by the olive tail moments (**Table 4**). Consistent with the DNA damaging ability, *T. bentzoë*
465 halted the cell cycle progression significantly ($p < 0.01$, *versus* control) in the G0/G1 phase (**Figure 2**).
466 A similar observation was reported in lung cancer cells, where casuarinin, a tannin purified from *T.*
467 *arjuna* L. bark, provoked apoptotic mechanism via DNA fragmentation and G0/G1 phase cell cycle
468 arrest [71].

469 It is noteworthy that, the cytotoxicity of the extract may arise from the complex interplay of the
470 cocktails of secondary metabolites present, which may act either synergistically or antagonistically to
471 produce the overall results. Also, crude extracts often comprised a pool of inactive phytoconstituents
472 that dilute the efficacy of the active components [72,73]. It is therefore of paramount importance to
473 purify and identify the principal bioactive components to conduct further mechanistic studies to
474 establish their molecular mode of action [72,74]. Moreover, isolating the lead compounds also allows
475 for the potential structural modification in an attempt to enhance their selectivity and potency [75].
476 As such, the MTT-guided fractionation revealed that only six out of the eleven preparative HPLC
477 subfractions retained the potent cytotoxicity of the crude extract (**Figure 3**). The HPLC subfraction
478 F6.1 was 1.4 folds more potent as compared to the crude extract.

479 LC-MS analysis in conjunction with NMR spectroscopy allowed the identification of 8 phenolic
480 compounds from the most bioactive subfraction F6. Punicalagin, isoterchebulin and ellagic acid have
481 been previously reported from the bark extract of the same species collected in Réunion Island [33].
482 Although, the other identified compounds are being reported for the first time, to the best of our
483 current knowledge, in *T. bentzoë* leaf, some were reported in the leaf extracts of other *Terminalia*

484 species. For instance, 2''-O-galloylvitexin and gallic acid were identified from *T. brachystemma* Welw.
 485 ex Hiern and *T. mollis* M. Laws leaves, respectively [35]. Likewise, terflavin A was found in *T.*
 486 *catappa* L. leaf [37].

487 Punicalagin and ellagic acid were reported to induce S Phase arrest and G0/G1 phase arrest in
 488 HepG2 cells, respectively [76]. Moreover, punicalagin induced G0/G1 phase arrest in papillary
 489 human thyroid carcinoma (BCPAP) cells via the NF- κ B signaling pathway [77]. In human ovarian
 490 cancer (A2780) cells, punicalagin treatment was associated with an increase in the number of cells
 491 arrested at G1/S phase as well as the downregulation of the β -catenin signaling pathway [78]. Ellagic
 492 acid administration in prostate cancer patients was associated with decreased prostate-specific
 493 antigen as well as reduced chemotherapy-induced myelotoxicity [79]. It may be strongly proposed
 494 that the overall cytotoxicity of *T. bentzoë* leaf extract may be a synergistic effect of the identified
 495 compounds. Gallic acid was reported to induce S phase arrest in HepG2 cells [80] and be cytotoxic to
 496 ovarian cancer cells [81]. Furthermore, gallic acid was also shown to impair centrosomal clustering
 497 in human cervical cancer (Hela) cells, thus causing a mitotic catastrophe and ultimate cell G2/M phase
 498 cell cycle arrest.

499 5. Conclusion

500 The findings evidenced the selective long-term cytotoxicity of the antioxidant-rich *T. bentzoë* leaf
 501 extract against HepG2 cells. This plant which is also used traditionally in the mitigation of asthma,
 502 haemorrhages, diarrhoea, and sexually transmissible diseases, amongst others, has also shown some
 503 *in-vitro* anticancer activities against HepG2 cells. The cytotoxic nature of *T. bentzoë* leaf extract against
 504 cancerous cells indicated that *T. bentzoë* leaf has the potential to be repurposed in the mitigation of
 505 cancer as part of traditional medicine. The results so far generated, supports the hypothesis that *T.*
 506 *bentzoë* extract induced apoptosis/necrosis cell death in HepG2 cells via the degradation of cellular
 507 genetic material and subsequent arrest of the cell cycle progression in G0/G1 phase. Overall, the MTT-
 508 guided fractionation of the crude extract allowed the characterisation of 10 phenolic compounds
 509 including punicalagin, ellagic acid, gallic acid, and methyl gallate that are known to have established
 510 *in vitro* and *in vivo* anticancer activities. However, the contribution of the other non-identified
 511 phytoconstituents cannot be excluded and thus further evaluation of identified components is
 512 warranted alongside the crude extract. The metabolite profiling of the leaf extract may be envisaged
 513 in future studies. This will allow to precisely ascribe the bioactive molecules present in *T. bentzoë* leaf.
 514 Taking into consideration the guidelines of the US national cancer institute as well as the selectivity
 515 index observed in this study, *T. bentzoë* leaf extract revealed as a promising candidate that can be
 516 exploited in the search for novel anticancer agents. The current study provided base line data for
 517 more in-depth investigations of the chemotherapeutic potential of *T. bentzoë* plant extracts. Further
 518 mechanistic investigation, directed towards delineating the molecular mechanisms via which the
 519 purified bioactive entities target of the aberrant signaling pathways involved in carcinogenesis, is
 520 needed to fuel *in-vivo* studies. Future animal studies and ideally human clinical trials are warranted
 521 to establish the physiological doses for human administration.

522 **Supplementary Materials:** Figure S1: Cell viability profile of HepG2 cells treated with *T. bentzoë* extract and
 523 fractions. Figure S2: Representatives annexin V-FITC/PI flow cytometric profile of HepG2 cells, 48 hours post
 524 extract/control treatment. Figure S3: Representatives cell cycle histogram of HepG2 cells, 48 hours post
 525 extract/control treatment. Figure S4: UPLC ESI MS of the butanol fraction 6 at the positive (A) and negative (B)
 526 mode. Figure S5: ¹H NMR spectrum (A) and HSQC spectrum (B) for punicalagin (1) in an HPLC fraction at RT
 527 2-3 min in methanol-d₄. Figure S6: ¹H NMR spectra for a mixture of isoterchebulin (2), terflavin A (3), and 3,4,6-
 528 trigalloyl-beta-D-glucopyranose (4) in a HPLC fraction at RT18-20 min in acetone-d₆ (A) and methanol-d₄ (B).
 529 Figure S7: ¹H NMR spectra for a mixture of 2''-O-galloyl-orientin (3) and 2''-O-galloyl-isoorientin (6) with a ratio
 530 of 5:2 based on the integration of single hydrogen in each compound. Figure S8: GC-MS chromatogram of TMSi
 531 derivatives of ethyl acetate (A) and butanol (B) fraction of *T. bentzoë*. Table S1 ¹H NMR spectral data (500 MHz,
 532 CD₃OD) of the O-galloyl-C-glycosylflavones 7 and 8 (5:2) [" in ppm, multiplicities and J values (Hz) are given in
 533 parentheses].

534 **Author Contributions:** Conceptualization, N.R and V.N; methodology, N.R., P.R, E.P., J.M., and T.D.; software,
 535 N.R., P.R, E.P., J.M., and T.D.; validation, N.R., P.R, E.P., J.M., and T.D.; formal analysis, N.R., P.R, E.P., J.M., and

536 T.D.; investigation, N.R., P.R, E.P., J.M., and T.D.; resources, E.B., T.B., W.L., and V.N.; data curation, N.R., P.R,
 537 E.P., J.M., and T.D.; writing—original draft preparation, N.R.; writing—review and editing, P.R, T.D., T.B., W.L.,
 538 E.B., and V.N.; visualization, N.R., E.P., J.M., and T.D.; supervision, T.B., W.L., and V.N.; project administration,
 539 T.B., V.N.; funding acquisition, T.B., W.L., and V.N. All authors have read and agreed to the published version
 540 of the manuscript.

541 **Acknowledgments:** We thank the director and staff of Alteo Group, Médine Sugar Estate and Mauritius
 542 National Park Conservation Services under the Ministry of Agro-Industry & Food Security, Mauritius, for
 543 permission to collect endemic plant samples and the Mauritius Herbarium for plant identification. This study
 544 was supported by the Royal Society and Royal Society of Chemistry international exchange award, Mauritius
 545 Research Council under the National Research and Innovation Chair Program studentship.

546 **Conflicts of interest:** The authors declare no conflict of interest.

547 References

- 548 1. Newman, D.J.; Cragg, G.M. Natural Products as Sources of New Drugs from 1981 to 2014. *J.*
 549 *Nat. Prod.* **2016**, *79*, 629–661, doi:10.1021/acs.jnatprod.5b01055.
- 550 2. Thomford, N.; Senthebane, D.; Rowe, A.; Munro, D.; Seele, P.; Maroyi, A.; Dzobo, K. Natural
 551 Products for Drug Discovery in the 21st Century: Innovations for Novel Drug Discovery. *Int.*
 552 *J. Mol. Sci.* **2018**, *19*, 1578–1607, doi:10.3390/ijms19061578.
- 553 3. Graham, J.G.; Quinn, M.L.; Fabricant, D.S.; Farnsworth, N.R. Plants used against cancer – an
 554 extension of the work of Jonathan Hartwell. *J. Ethnopharmacol.* **2000**, *73*, 347–377,
 555 doi:10.1016/S0378-8741(00)00341-X.
- 556 4. Willis, K.J. *State of the World's Plants 2017. Report. Royal Botanic Gardens, Kew.*; 2017;
- 557 5. Ang, L.; Song, E.; Lee, H.W.; Lee, M.S. Herbal Medicine for the Treatment of Coronavirus
 558 Disease 2019 (COVID-19): A Systematic Review and Meta-Analysis of Randomized
 559 Controlled Trials. *J. Clin. Med.* **2020**, *9*, 1583, doi:10.3390/jcm9051583.
- 560 6. Ang, L.; Lee, H.W.; Kim, A.; Lee, M.S. Herbal medicine for the management of COVID-19
 561 during the medical observation period: A review of guidelines. *Integr. Med. Res.* **2020**, *9*,
 562 100465, doi:10.1016/j.imr.2020.100465.
- 563 7. Panyod, S.; Ho, C.-T.; Sheen, L.-Y. Dietary therapy and herbal medicine for COVID-19
 564 prevention: A review and perspective. *J. Tradit. Complement. Med.* **2020**, *10*, 420–427,
 565 doi:10.1016/j.jtcme.2020.05.004.
- 566 8. Myers, N.; Mittermeier, R.A.; Mittermeier, C.G.; da Fonseca, G.A.B.; Kent, J. Biodiversity
 567 hotspots for conservation priorities. *Nature* **2000**, *403*, 853–858, doi:10.1038/35002501.
- 568 9. Kinghorn, A.D.; Farnsworth, N.R.; Soejarto, D.D.; Cordell, G.A.; Pezzuto, J.M.; Udeani, G.O.;
 569 Wani, M.C.; Wall, M.E.; Navarro, H.A.; Kramer, R.A.; et al. Novel Strategies for the Discovery
 570 of Plant-Derived Anticancer Agents. *Pure Appl. Chem.* **1999**, *71*, 1611–1618.
- 571 10. Kinghorn, A.D.; De Blanco, E.J.C.; Lucas, D.M.; Rakotondraibe, H.L.; Orjala, J.; Soejarto, D.D.;
 572 Oberlies, N.H.; Pearce, C.J.; Wani, M.C.; Stockwell, B.R.; et al. Discovery of Anticancer Agents
 573 of Diverse Natural Origin. *Anticancer Res.* **2016**, *36*, 5623–5638, doi:10.21873/anticancer.11146.
- 574 11. Rasoanaivo, P. Rain Forests of Madagascar : Sources of Industrial and Medicinal Plants. *Ambio*
 575 **1990**, *19*, 421–424.
- 576 12. Das, A.; Sarkar, S.; Bhattacharyya, S.; Gantait, S. Biotechnological advancements in
 577 *Catharanthus roseus* (L.) G. Don. *Appl. Microbiol. Biotechnol.* **2020**, *104*, 4811–4835,
 578 doi:10.1007/s00253-020-10592-1.
- 579 13. Alam, P.; Sharaf-Eldin, M. Limited Production Of Plant Derived Anticancer Drugs Vinblastine
 580 And Vincristine. *Planta Med.* **2016**, *82*, doi:10.1055/s-0036-1578706.

- 581 14. Garot, E.; Joët, T.; Combes, M.-C.; Lashermes, P. Genetic diversity and population divergences
582 of an indigenous tree (*Coffea mauritiana*) in Reunion Island: role of climatic and geographical
583 factors. *Heredity (Edinb)*. **2019**, *122*, 833–847, doi:10.1038/s41437-018-0168-9.
- 584 15. Baider, C.; Florens, F.B.V.; Baret, S.; Beaver, K.; Strasberg, D.; Kueffer, C. Status of plant
585 conservation in oceanic islands of the Western Indian Ocean. *Proc. 4th Glob. Bot. Gard. Congr.*
586 **2010**, 1–7.
- 587 16. Rummun, N.; Neergheen-Bhujun, V.S.; Pynee, K.B.; Baider, C.; Bahorun, T. The role of
588 endemic plants in Mauritian traditional medicine – Potential therapeutic benefits or placebo
589 effect? *J. Ethnopharmacol.* **2018**, *213*, 111–117, doi:10.1016/j.jep.2017.10.006.
- 590 17. Humphreys, A.M.; Govaerts, R.; Ficinski, S.Z.; Nic Lughadha, E.; Vorontsova, M.S. Global
591 dataset shows geography and life form predict modern plant extinction and rediscovery. *Nat.*
592 *Ecol. Evol.* **2019**, *3*, 1043–1047, doi:10.1038/s41559-019-0906-2.
- 593 18. Page, W. *Terminalia benzoin* ssp. *benzoin*. The IUCN Red List of Threatened Species. **1998**,
594 8235, e.T30745A9575875, doi:10.2305/IUCN.UK.1998.RLTS.T30745A9575875.en.
- 595 19. Mileo, A.M.; Miccadei, S. Polyphenols as Modulator of Oxidative Stress in Cancer Disease:
596 New Therapeutic Strategies. *Oxid. Med. Cell. Longev.* **2016**, *2016*, 1–17,
597 doi:10.1155/2016/6475624.
- 598 20. Khan, H.; Reale, M.; Ullah, H.; Sureda, A.; Tejada, S.; Wang, Y.; Zhang, Z.-J.; Xiao, J. Anti-
599 cancer effects of polyphenols via targeting p53 signaling pathway: updates and future
600 directions. *Biotechnol. Adv.* **2020**, *38*, 107385, doi:10.1016/j.biotechadv.2019.04.007.
- 601 21. Azqueta, A.; Collins, A. Polyphenols and DNA Damage: A Mixed Blessing. *Nutrients* **2016**, *8*,
602 785, doi:10.3390/nu8120785.
- 603 22. Niedzwiecki, A.; Roomi, M.W.; Kalinovskiy, T.; Rath, M. Anticancer efficacy of polyphenols
604 and their combinations. *Nutrients* **2016**, *8*, doi:10.3390/nu8090552.
- 605 23. Page, W.; D'Argent, G. *A vegetation survey of Mauritius (Indian Ocean) to identify priority*
606 *rainforest areas for conservation management*; 1997.
- 607 24. Rummun, N.; Somanah, J.; Ramsaha, S.; Bahorun, T.; Neergheen-Bhujun, V.S. Bioactivity of
608 Nonedible Parts of *Punica granatum* L.: A Potential Source of Functional Ingredients. *Int. J.*
609 *Food Sci.* **2013**, *2013*, 1–12, doi:10.1155/2013/602312.
- 610 25. Rummun, N.; Hughes, R.E.; Beesoo, R.; Li, W.W.; Aldulaimi, O.; Macleod, K.G.; Bahorun, T.;
611 Carragher, N.O.; Kagansky, A.; Neergheen-Bhujun, V.S. Mauritian Endemic Medicinal Plant
612 Extracts Induce G2/M Phase Cell Cycle Arrest and Growth Inhibition of Oesophageal
613 Squamous Cell Carcinoma in Vitro. *Acta Naturae* **2019**, *11*, 81–90, doi:10.32607/20758251-2019-
614 11-1-81-90.
- 615 26. Ramful, D.; Tarnus, E.; Rondeau, P.; Robert Da Silva, C.; Bahorun, T.; Bourdon, E. Citrus fruit
616 extracts reduce advanced glycation end products (AGEs)- and H₂O₂-induced oxidative stress
617 in human adipocytes. *J. Agric. Food Chem.* **2010**, *58*, 11119–11129, doi:10.1021/jf102762s.
- 618 27. Al-Dabbagh, B.; Elhaty, I.A.; Al Hrouf, A.; Al Sakkaf, R.; El-Awady, R.; Ashraf, S.S.; Amin, A.
619 Antioxidant and anticancer activities of *Trigonella foenum-graecum*, *Cassia acutifolia* and
620 *Rhazya stricta*. *BMC Complement. Altern. Med.* **2018**, *18*, 240, doi:10.1186/s12906-018-2285-7.
- 621 28. Franken, N.A.P.; Rodermond, H.M.; Stap, J.; Haveman, J.; van Bree, C. Clonogenic assay of
622 cells in vitro. *Nat. Protoc.* **2006**, *1*, 2315–2319, doi:10.1038/nprot.2006.339.
- 623 29. Collins, A.R. The Comet Assay for DNA Damage and Repair: Principles, Applications, and

- 624 Limitations. *Mol. Biotechnol.* **2004**, *26*, 249–261, doi:10.1385/MB:26:3:249.
- 625 30. Miyaji, C.; Jordão, B.; Ribeiro, L.; Eira, A.; Cólus, I. Genotoxicity and antigenotoxicity
626 assessment of shiitake (*Lentinula edodes* (Berkeley) Pegler) using the Comet assay. *Genet. Mol.*
627 *Biol.* **2004**, *27*, 108–114, doi:10.1590/S1415-47572004000100018.
- 628 31. Catan, A.; Turpin, C.; Diotel, N.; Patche, J.; Guerin-Dubourg, A.; Debussche, X.; Bourdon, E.;
629 Ah-You, N.; Le Moullec, N.; Besnard, M.; et al. Aging and glycation promote erythrocyte
630 phagocytosis by human endothelial cells: Potential impact in atherothrombosis under diabetic
631 conditions. *Atherosclerosis* **2019**, *291*, 87–98, doi:10.1016/j.atherosclerosis.2019.10.015.
- 632 32. Bai, J.; Cederbaum, A.I. Cycloheximide Protects HepG2 Cells from Serum Withdrawal-
633 Induced Apoptosis by Decreasing p53 and Phosphorylated p53 Levels. *J. Pharmacol. Exp. Ther.*
634 **2006**, *319*, 1435–1443, doi:10.1124/jpet.106.110007.
- 635 33. Apel, C.; Bignon, J.; Garcia-Alvarez, M.C.; Ciccone, S.; Clerc, P.; Grondin, I.; Girard-
636 Valenciennes, E.; Smadja, J.; Lopes, P.; Frédérick, M.; et al. N-myristoyltransferases inhibitory
637 activity of ellagitannins from *Terminalia bentzoë* (L.) L. f. subsp. *bentzoë*. *Fitoterapia* **2018**, *131*,
638 91–95, doi:10.1016/j.fitote.2018.10.014.
- 639 34. Latté, K.P.; Ferreira, D.; Venkatraman, M.S.; Kolodziej, H. O-galloyl-C-glycosylflavones from
640 *Pelargonium reniforme*. *Phytochemistry* **2002**, *59*, 419–424, doi:10.1016/S0031-9422(01)00403-4.
- 641 35. Liu, M.; Katerere, D.R.; Gray, A.I.; Seidel, V. Phytochemical and antifungal studies on
642 *Terminalia mollis* and *Terminalia brachystemma*. *Fitoterapia* **2009**, *80*, 369–373,
643 doi:10.1016/j.fitote.2009.05.006.
- 644 36. Marzouk, M.S.A.; El-Toumy, S.A.A.; Moharram, F.A. Pharmacologically Active Ellagitannins
645 from *Terminalia myriocarpa*. *Planta Med.* **2002**, *68*, 523–527, doi:10.1055/s-2002-32549.
- 646 37. Tanaka, T.; NONAKA, G.-I.; NISHIOKA, I. Tannins and related compounds. XLII. Isolation
647 and characterization of four new hydrolyzable tannins, terflavins A and B, tergallagin and
648 tercatatin from the leaves of *Terminalia catappa* L. *Chem. Pharm. Bull. (Tokyo)*. **1986**, *34*, 1039–
649 1049, doi:10.1248/cpb.34.1039.
- 650 38. Yakubu, O.F.; Adebayo, A.H.; Dokunmu, T.M.; Zhang, Y.-J.; Iweala, E.E.J. Cytotoxic Effects of
651 Compounds Isolated from *Ricinodendron heudelotii*. *Molecules* **2019**, *24*, 145,
652 doi:10.3390/molecules24010145.
- 653 39. Brower, V. Back to Nature: Extinction of Medicinal Plants Threatens Drug Discovery. *JNCI J.*
654 *Natl. Cancer Inst.* **2008**, *100*, 838–839, doi:10.1093/jnci/djn199.
- 655 40. Anand, U.; Jacobo-Herrera, N.; Altemimi, A.; Lakhssassi, N. A comprehensive review on
656 medicinal plants as antimicrobial therapeutics: Potential avenues of biocompatible drug
657 discovery. *Metabolites* **2019**, *9*, 1–13, doi:10.3390/metabo9110258.
- 658 41. Ferreyra, F.M.L.; Rius, S.P.; Casati, P. Flavonoids: biosynthesis, biological functions, and
659 biotechnological applications. *Front. Plant Sci.* **2012**, *3*, 1–15, doi:10.3389/fpls.2012.00222.
- 660 42. Baborun, T.; Ramful-Baboolall, D.; Neergheen-Bhujun, V.; Aruoma, O.I.; Kumar, A.; Verma,
661 S.; Tarnus, E.; Da Silva, C.R.; Rondeau, P.; Bourdon, E. Phytochemical Nutrients in Citrus:
662 Biochemical and Molecular Evidence. In *Advances in Citrus Nutrition*; Srivastava, A.K., Ed.;
663 Springer Netherlands: Dordrecht, 2012; Vol. 9789400741, pp. 25–40 ISBN 978-94-007-4170-6.
- 664 43. Perillo, B.; Di Donato, M.; Pezone, A.; Di Zazzo, E.; Giovannelli, P.; Galasso, G.; Castoria, G.;
665 Migliaccio, A. ROS in cancer therapy: the bright side of the moon. *Exp. Mol. Med.* **2020**, *52*,
666 192–203, doi:10.1038/s12276-020-0384-2.

- 667 44. Ashraf, M.A. Phytochemicals as Potential Anticancer Drugs: Time to Ponder Nature's Bounty.
668 *Biomed Res. Int.* **2020**, *2020*, 1–7, doi:10.1155/2020/8602879.
- 669 45. Li, W.-Y.; Chan, S.-W.; Guo, D.-J.; Yu, P.H.-F. Correlation Between Antioxidative Power and
670 Anticancer Activity in Herbs from Traditional Chinese Medicine Formulae with Anticancer
671 Therapeutic Effect. *Pharm. Biol.* **2007**, *45*, 541–546, doi:10.1080/13880200701498879.
- 672 46. Sammar, M.; Abu-Farich, B.; Rayan, I.; Falah, M.; Rayan, A. Correlation between cytotoxicity
673 in cancer cells and free radical-scavenging activity: *In vitro* evaluation of 57 medicinal and
674 edible plant extracts. *Oncol. Lett.* **2019**, *18*, 6563–6571, doi:10.3892/ol.2019.11054.
- 675 47. Snezhkina, A. V.; Kudryavtseva, A. V.; Kardymon, O.L.; Savvateeva, M. V.; Melnikova, N. V.;
676 Krasnov, G.S.; Dmitriev, A.A. ROS Generation and Antioxidant Defense Systems in Normal
677 and Malignant Cells. *Oxid. Med. Cell. Longev.* **2019**, *2019*, 1–17, doi:10.1155/2019/6175804.
- 678 48. Aggarwal, V.; Tuli, H.S.; Varol, A.; Thakral, F.; Yerer, M.B.; Sak, K.; Varol, M.; Jain, A.; Khan,
679 M.A.; Sethi, G. Role of Reactive Oxygen Species in Cancer Progression: Molecular
680 Mechanisms and Recent Advancements. *Biomolecules* **2019**, *9*, 735, doi:10.3390/biom9110735.
- 681 49. Panieri, E.; Santoro, M.M. Ros homeostasis and metabolism: A dangerous liason in cancer
682 cells. *Cell Death Dis.* **2016**, *7*, 1–12, doi:10.1038/cddis.2016.105.
- 683 50. Gorrini, C.; Harris, I.S.; Mak, T.W. Modulation of oxidative stress as an anticancer strategy.
684 *Nat. Rev. Drug Discov.* **2013**, *12*, 931–947, doi:10.1038/nrd4002.
- 685 51. Procházková, D.; Boušová, I.; Wilhelmová, N. Antioxidant and prooxidant properties of
686 flavonoids. *Fitoterapia* **2011**, *82*, 513–523, doi:10.1016/j.fitote.2011.01.018.
- 687 52. Moulisha, B.; Ashok Kumar, G.; Pallab Kanti, H. Anti-leishmanial and anti-cancer activities of
688 a pentacyclic triterpenoid isolated from the leaves of Terminalia arjuna Combretaceae. *Trop.*
689 *J. Pharm. Res.* **2010**, *9*, 135–140, doi:10.4314/tjpr.v9i2.53700.
- 690 53. Shankara, R.B.; Ramachandra, Y.; Rajan, S.S.; Sujana Ganapathy, P.; Yarla, N.; Richard, S.;
691 Dhananjaya, B. Evaluating the anticancer potential of ethanolic gall extract of Terminalia
692 chebula (Gaertn.) Retz. (combretaceae). *Pharmacognosy Res.* **2016**, *8*, 209, doi:10.4103/0974-
693 8490.182919.
- 694 54. Shanehbandi, D.; Zarredar, H.; Asadi, M.; Zafari, V.; Esmaeili, S.; Seyedrezazadeh, E.;
695 Soleimani, Z.; Sabagh Jadid, H.; Eyvazi, S.; Feyziniya, S.; et al. Anticancer Impacts of
696 Terminalia catappa Extract on SW480 Colorectal Neoplasm Cell Line. *J. Gastrointest. Cancer*
697 **2019**, doi:10.1007/s12029-019-00349-z.
- 698 55. Ramos-Silva, A.; Tavares-Carreón, F.; Figueroa, M.; De la Torre-Zavala, S.; Gastelum-
699 Arellanez, A.; Rodríguez-García, A.; Galán-Wong, L.J.; Avilés-Arnaut, H. Anticancer potential
700 of Thevetia peruviana fruit methanolic extract. *BMC Complement. Altern. Med.* **2017**, *17*, 241,
701 doi:10.1186/s12906-017-1727-y.
- 702 56. Vijayarathna, S.; Sasidharan, S. Cytotoxicity of methanol extracts of Elaeis guineensis on MCF-
703 7 and Vero cell lines. *Asian Pac. J. Trop. Biomed.* **2012**, *2*, 826–829, doi:10.1016/S2221-
704 1691(12)60237-8.
- 705 57. Mirzayans, R.; Andrais, B.; Murray, D. Viability Assessment Following Anticancer Treatment
706 Requires Single-Cell Visualization. *Cancers (Basel)*. **2018**, *10*, 255, doi:10.3390/cancers10080255.
- 707 58. Jahanban-Esfahlan, R.; Seidi, K.; Manjili, M.H.; Jahanban-Esfahlan, A.; Javaheri, T.; Zare, P.
708 Tumor Cell Dormancy: Threat or Opportunity in the Fight against Cancer. *Cancers (Basel)*.
709 **2019**, *11*, 1–23, doi:10.3390/cancers11081207.

- 710 59. Mirzayans, R.; Murray, D. Intratumor Heterogeneity and Therapy Resistance: Contributions
711 of Dormancy, Apoptosis Reversal (Anastasis) and Cell Fusion to Disease Recurrence. *Int. J.*
712 *Mol. Sci.* **2020**, *21*, 1308, doi:10.3390/ijms21041308.
- 713 60. Myint, P.P.; Dao, T.T.P.; Kim, Y.S. Anticancer Activity of *Smallanthus sonchifolius* Methanol
714 Extract against Human Hepatocellular Carcinoma Cells. *Molecules* **2019**, *24*, 3054,
715 doi:10.3390/molecules24173054.
- 716 61. Khorsandi, K.; Kianmehr, Z.; Hosseinmardi, Z.; Hosseinzadeh, R. Anti-cancer effect of gallic
717 acid in presence of low level laser irradiation: ROS production and induction of apoptosis and
718 ferroptosis. *Cancer Cell Int.* **2020**, *20*, 18, doi:10.1186/s12935-020-1100-y.
- 719 62. Afsar, T.; Trembley, J.H.; Salomon, C.E.; Razak, S.; Khan, M.R.; Ahmed, K. Growth inhibition
720 and apoptosis in cancer cells induced by polyphenolic compounds of *Acacia hydaspica*:
721 Involvement of multiple signal transduction pathways. *Sci. Rep.* **2016**, *6*,
722 doi:10.1038/srep23077.
- 723 63. Silva, M.T. Secondary necrosis: The natural outcome of the complete apoptotic program. *FEBS*
724 *Lett.* **2010**, *584*, 4491–4499, doi:10.1016/j.febslet.2010.10.046.
- 725 64. Lee, S.Y.; Ju, M.K.; Jeon, H.M.; Jeong, E.K.; Lee, Y.J.; Kim, C.H.; Park, H.G.; Han, S.I.; Kang,
726 H.S. Regulation of Tumor Progression by Programmed Necrosis. *Oxid. Med. Cell. Longev.* **2018**,
727 *2018*, 1–28, doi:10.1155/2018/3537471.
- 728 65. Edderkaoui, M.; Odinokova, I.; Ohno, I.; Gukovsky, I.; Go, V.L.W.; Pandol, S.J.; Gukovskaya,
729 A.S. Ellagic acid induces apoptosis through inhibition of nuclear factor kB in pancreatic cancer
730 cells. *World J. Gastroenterol.* **2008**, *14*, 3672, doi:10.3748/wjg.14.3672.
- 731 66. Grace Nirmala, J.; Evangeline Celsia, S.; Swaminathan, A.; Narendhirakannan, R.T.;
732 Chatterjee, S. Cytotoxicity and apoptotic cell death induced by *Vitis vinifera* peel and seed
733 extracts in A431 skin cancer cells. *Cytotechnology* **2018**, *70*, 537–554, doi:10.1007/s10616-017-
734 0125-0.
- 735 67. Mahassni, S.H.; Al-Reemi, R.M. Apoptosis and necrosis of human breast cancer cells by an
736 aqueous extract of garden cress (*Lepidium sativum*) seeds. *Saudi J. Biol. Sci.* **2013**, *20*, 131–139,
737 doi:10.1016/j.sjbs.2012.12.002.
- 738 68. Moreira, H.; Szyjka, A.; Paliszkiewicz, K.; Barg, E. Prooxidative Activity of Celastrol Induces
739 Apoptosis, DNA Damage, and Cell Cycle Arrest in Drug-Resistant Human Colon Cancer
740 Cells. *Oxid. Med. Cell. Longev.* **2019**, *2019*, 1–12, doi:10.1155/2019/6793957.
- 741 69. Chen, X.; Song, L.; Hou, Y.; Li, F. Reactive oxygen species induced by icaritin promote DNA
742 strand breaks and apoptosis in human cervical cancer cells. *Oncol. Rep.* **2019**, *41*, 765–778,
743 doi:10.3892/or.2018.6864.
- 744 70. Augustine, D.; Rao, R.S.; Anbu, J.; Chidambara Murthy, K.N. In vitro cytotoxic and apoptotic
745 induction effect of earthworm coelomic fluid of *Eudrilus eugeniae*, *Eisenia foetida*, and
746 *Perionyx excavatus* on human oral squamous cell carcinoma-9 cell line. *Toxicol. Reports* **2019**,
747 *6*, 347–357, doi:10.1016/j.toxrep.2019.04.005.
- 748 71. Kuo, P.-L.; Hsu, Y.-L.; Lin, T.-C.; Chang, J.-K.; Lin, C.-C. Induction of cell cycle arrest and
749 apoptosis in human non-small cell lung cancer A549 cells by casuarinin from the bark of
750 *Terminalia arjuna* Linn. *Anticancer. Drugs* **2005**, *16*, 409–415, doi:10.1097/00001813-200504000-
751 00007.
- 752 72. Atanasov, A.G.; Waltenberger, B.; Pferschy-Wenzig, E.-M.; Linder, T.; Wawrosch, C.; Uhrin,

- 753 P.; Temml, V.; Wang, L.; Schwaiger, S.; Heiss, E.H.; et al. Discovery and resupply of
754 pharmacologically active plant-derived natural products: A review. *Biotechnol. Adv.* **2015**, *33*,
755 1582–1614, doi:10.1016/j.biotechadv.2015.08.001.
- 756 73. Chikezie, P.C.; Ibegbulem, C.O.; Mbagwu, F.N. Bioactive principles from medicinal plants.
757 *Res. J. Phytochem.* **2015**, *9*, 88–115, doi:10.3923/rjphyto.2015.88.115.
- 758 74. Katiyar, C.; Kanjilal, S.; Gupta, A.; Katiyar, S. Drug discovery from plant sources: An
759 integrated approach. *AYU (An Int. Q. J. Res. Ayurveda)* **2012**, *33*, 10, doi:10.4103/0974-
760 8520.100295.
- 761 75. Liu, Z. Preparation of Botanical Samples for Biomedical Research. *Endocrine, Metab. Immune*
762 *Disord. Targets* **2008**, *8*, 112–121, doi:10.2174/187153008784534358.
- 763 76. Li, J.; Wang, G.; Hou, C.; Li, J.; Luo, Y.; Li, B. Punicalagin and ellagic acid from pomegranate
764 peel induce apoptosis and inhibits proliferation in human HepG2 hepatoma cells through
765 targeting mitochondria. *Food Agric. Immunol.* **2019**, *30*, 897–912,
766 doi:10.1080/09540105.2019.1642857.
- 767 77. Cheng, X.; Yao, X.; Xu, S.; Pan, J.; Yu, H.; Bao, J.; Guan, H.; Lu, R.; Zhang, L. Punicalagin
768 induces senescent growth arrest in human papillary thyroid carcinoma BCPAP cells via NF-
769 κ B signaling pathway. *Biomed. Pharmacother.* **2018**, *103*, 490–498,
770 doi:10.1016/j.biopha.2018.04.074.
- 771 78. Tang, J.M.; Min, J.; Li, B.S.; Hong, S.S.; Liu, C.; Hu, M.; Li, Y.; Yang, J.; Hong, L. Therapeutic
772 Effects of Punicalagin Against Ovarian Carcinoma Cells in Association with β -Catenin
773 Signaling Inhibition. *Int. J. Gynecol. Cancer* **2016**, *26*, 1557–1563,
774 doi:10.1097/IGC.0000000000000805.
- 775 79. Ceci, C.; Lacal, P.M.; Tentori, L.; De Martino, M.G.; Miano, R.; Graziani, G. Experimental
776 evidence of the antitumor, antimetastatic and antiangiogenic activity of ellagic acid. *Nutrients*
777 **2018**, *10*, 1–23, doi:10.3390/nu10111756.
- 778 80. Sánchez-Carranza, J.; Alvarez, L.; Marquina-Bahena, S.; Salas-Vidal, E.; Cuevas, V.; Jiménez,
779 E.; Veloz G., R.; Carraz, M.; González-Maya, L. Phenolic Compounds Isolated from
780 *Caesalpinia coriaria* Induce S and G2/M Phase Cell Cycle Arrest Differentially and Trigger
781 Cell Death by Interfering with Microtubule Dynamics in Cancer Cell Lines. *Molecules* **2017**, *22*,
782 666, doi:10.3390/molecules22040666.
- 783 81. Johnson-ajinwo, O.R.; Richardson, A.; Li, W.-W. Cytotoxic effects of stem bark extracts and
784 pure compounds from *Margaritaria discoidea* on human ovarian cancer cell lines.
785 *Phytomedicine* **2015**, *22*, 1–4, doi:10.1016/j.phymed.2014.09.008.
- 786
787
788